

Near-field light emission from nano- and micrometric complex structures

M. Pieruccini

*CNR, Istituto per i Processi Chimico-Fisici Sez. Messina,
Via La Farina 237, I-98123 Messina, Italy*

S. Savasta and R. Girlanda

*Istituto Nazionale per la Fisica della Materia (INFN) and
Dipartimento di Fisica della Materia e Tecnologie Fisiche Avanzate,
Università di Messina Salita Sperone 31, I-98166 Messina, Italy*

R. C. Iotti, and F. Rossi

*Istituto Nazionale per la Fisica della Materia (INFN) and Dipartimento di Fisica,
Politecnico di Torino, Corso Duca degli Abruzzi 24, 10129 Torino, Italy*

(Dated: February 1, 2008)

Abstract

We propose a general theoretical scheme for the investigation of light emitted from nano- and micrometric structures of arbitrary shape and composition. More specifically, the proposed fully three-dimensional approach allows to derive the light-intensity distributions around the emitting structures and their modifications in the presence of nearby scattering objects. Our analysis allows to better identify the non-trivial relationship between near-field images and fluorescent objects.

PACS numbers: 78.67.-n, 42.50.Ct, 07.79.Lh

Recent continuous progress in scanning near-field microscopy together with the development of adequate nanofabrication techniques has enhanced our insight into the field distributions in the proximity of nano- and microstructured materials. This insight is of great relevance for the design of future optical circuitry able to process light with the versatility of electronic chips. These developments have stimulated more refined theoretical approaches as well as novel simulation strategies for the analysis of light propagation in complex structures and have renewed the interest in the classical theory of light scattering [1, 2]. Indeed, theoretical predictions are essential for the design of photonic structures able to control the propagation of light. As a matter of fact, most of the theoretical investigations performed so far focus on the scattering of incident light illuminating structures of non-trivial shapes [1, 3], or study light modes in photonic crystals and microcavities [4]. However, optical circuitry, besides passive elements controlling/manipulating the flow of photons, require active components able to emit and/or amplify light. This, in turn, opens relevant questions concerning the emission patterns of active mesoscopic systems: Which is the actual field distribution around emitting structures? How does the interaction with nearby scattering objects modify the field distribution? What kind of relationship between near-field images and fluorescent objects holds?

Aim of this Letter is to provide a general theoretical framework for the evaluation of the field distributions in the proximity of three-dimensional (3D) mesoscopic fluorescent objects in the presence of nearby scattering structures. The proposed quantum theory of light emission can be applied to a great variety of nanostructured optically active materials as mesoscopic dielectric objects uniformly doped with optically active molecules (e.g., dye molecules) or embedding semiconductor dots or layers able to emit light when appropriately excited.

As a starting point, let us consider the key quantity we want to investigate, i.e., the spectrally-resolved energy density $\mathcal{I}(\mathbf{r}, \omega)$ corresponding to the electric field at point \mathbf{r} ; this can be defined as:

$$\frac{\varepsilon_0}{2} \left\langle \hat{\mathbf{E}}^-(\mathbf{r}, \omega) \cdot \hat{\mathbf{E}}^+(\mathbf{r}, \omega') \right\rangle = \mathcal{I}(\mathbf{r}, \omega) \delta(\omega - \omega') , \quad (1)$$

where $\hat{\mathbf{E}}^+(\mathbf{r}, \omega)$ is the electric-field operator corresponding to the positive frequency ω (it can be expanded in terms of photon destruction operators) and $\hat{\mathbf{E}}^-(\mathbf{r}, \omega)$ is its Hermitian conjugate. Our theoretical approach is based on the Green's tensor technique in the frequency

domain [1, 5]. The electric field operator at a given positive frequency can be regarded as the sum of scattering and emission contributions [5]:

$$\hat{\mathbf{E}}^+(\mathbf{r}, \omega) = \hat{\mathbf{E}}_s^+(\mathbf{r}, \omega) + \hat{\mathbf{E}}_e^+(\mathbf{r}, \omega) . \quad (2)$$

The first term describes light coming from free-space and scattered by the material system, i.e.,

$$\hat{\mathbf{E}}_s^+(\mathbf{r}, \omega) = \hat{\mathbf{E}}_0^+(\mathbf{r}, \omega) - k^2 \int \vec{\mathbf{G}}(\mathbf{r}, \mathbf{r}', \omega) \chi(\mathbf{r}', \omega) \hat{\mathbf{E}}_0^+(\mathbf{r}', \omega) d\mathbf{r}' , \quad (3)$$

where $k = \omega/c$, the free-space electric-field operator $\hat{\mathbf{E}}_0^+$ describes input light, and $\chi = \varepsilon - 1$ is the susceptibility function of the material system (that we have assumed to be a local and scalar function to avoid complications), and $\vec{\mathbf{G}}$ is the Green tensor obeying the following equation

$$-\nabla \times \nabla \times \vec{\mathbf{G}}(\mathbf{r}, \mathbf{r}', \omega) + k^2 \varepsilon(\mathbf{r}, \omega) \vec{\mathbf{G}}(\mathbf{r}, \mathbf{r}', \omega) = \mathbf{I} \delta(\mathbf{r}, \mathbf{r}') , \quad (4)$$

where \mathbf{I} is the unit dyadic. We stress that nonlocality and/or anisotropy can be easily implemented [5]. The second term in Eq. (2) describes light emitted by the material system itself, i.e.,

$$\hat{\mathbf{E}}_e^+(\mathbf{r}, \omega) = -i\omega\mu_0 \int \vec{\mathbf{G}}(\mathbf{r}, \mathbf{r}', \omega) \hat{\mathbf{j}}(\mathbf{r}', \omega) d\mathbf{r}' , \quad (5)$$

where the integration is performed over the volume of the scattering system and μ_0 denotes the magnetic permeability of vacuum. Here, the quantum noise operators $\hat{\mathbf{j}}$ are the sources of spontaneous light emission. These zero-mean operators can be derived from the Heisenberg-Langevin equations for the material system [6] and are present only if the susceptibility tensor describing the material system has an imaginary part; they are a direct consequence of the fluctuation-dissipation theorem and obey the following commutation rules:[5]

$$\left[\hat{j}_l(\mathbf{r}, \omega), \hat{j}_{l'}(\mathbf{r}', \omega) \right] = 0 , \quad (6)$$

$$\left[\hat{j}_l(\mathbf{r}, \omega), \hat{j}_{l'}^\dagger(\mathbf{r}', \omega) \right] = \frac{\hbar}{\pi\mu_0} \frac{\omega^2}{c^2} |\chi^I(\mathbf{r}, \omega)| \delta_{ll'} \delta(\mathbf{r} - \mathbf{r}') \delta(\omega - \omega') , \quad (7)$$

where χ^I indicates the imaginary part of χ . By inserting Eq. (2) into Eq. (1), it is easy to verify that the intensity of the emitted light is directly related to the correlation function of quantum noise currents: $\langle \hat{\mathbf{j}}^\dagger \cdot \hat{\mathbf{j}} \rangle$. In order to calculate it explicitly we adopt a simple 2-level molecular model to describe the dielectric function of the scattering system,

$$\chi(\mathbf{r}, \omega) = \chi_s(\mathbf{r}) + \mathcal{N}(\mathbf{r}) \frac{d^2}{\varepsilon_0 \hbar} \frac{N_a(\mathbf{r}) - N_b(\mathbf{r})}{\omega_0 - \omega + i\gamma} , \quad (8)$$

FIG. 1: (a) Field-intensity distribution around a pair of nanoscopic emitting quavers with uniform composition and population densities; (b) as (a) but with the elliptic pad on the right of the structure replaced with a silver pad. The two calculations have been made at $\lambda = 600$ nm and on the observation plane located 30 nm above the structure.

where χ_s is the real susceptibility of the scattering system in the absence of active molecules, d is the transition dipole moment, \mathcal{N} gives the density of active molecules, and $N_{a(b)}$ indicates the population densities of the upper (a) and lower (b) levels. This simple model can be easily extended to include non-random molecular orientations, more energy levels and molecular species. Also more complex models describing, e.g., semiconductor dielectric functions, [6] can be adopted. By using this simple model we obtain,

$$\left\langle \hat{j}_l^\dagger(\mathbf{r}, \omega) \hat{j}_{l'}(\mathbf{r}', \omega') \right\rangle = \frac{\hbar}{\pi \mu_0} \frac{\omega^2}{c^2} \chi^I(\mathbf{r}, \omega) N(\mathbf{r}) \delta_{ll'} \delta(\mathbf{r} - \mathbf{r}') \delta(\omega - \omega'), \quad (9)$$

with the population factor $N(\mathbf{r}) = N_a(\mathbf{r}) / (N_b(\mathbf{r}) - N_a(\mathbf{r}))$. In the following we consider the case of absence of input photons ($\langle \mathbf{E}_0^-(\mathbf{r}, \omega) \cdot \mathbf{E}_0^+(\mathbf{r}, \omega') \rangle = 0$). By combining Eqs. (2) and

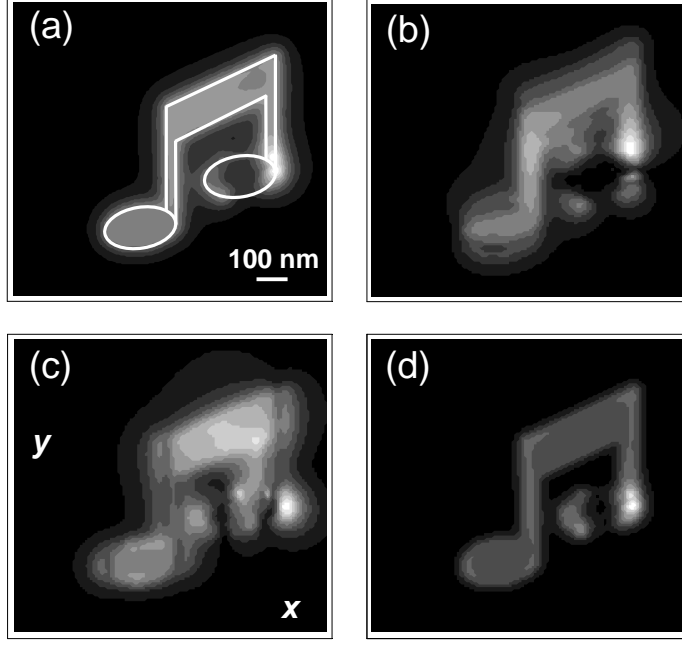


FIG. 2: (a) Field-intensity distribution around a pair of nanoscopic emitting quavers with uniform composition and population densities; (b) as (a) but with the elliptic pad on the right of the structure replaced with a silver pad. The two calculations have been made at $\lambda = 600$ nm and on the observation plane located 30 nm above the structure.

(9), we obtain $\mathcal{I}(\mathbf{r}, \omega) = \sum_l \mathcal{I}_l(\mathbf{r}, \omega)$ with

$$\mathcal{I}_l(\mathbf{r}, \omega) = \frac{\hbar k^4}{2\pi} \sum_{\nu'} \int N(\mathbf{r}') \varepsilon^I(\mathbf{r}', \omega) |G_{l\nu'}(\mathbf{r}, \mathbf{r}', \omega)|^2 d\mathbf{r}' . \quad (10)$$

We observe that population densities in principle are affected by light emission, thus Eq. (10) should be solved self-consistently together with the rate equations for the populations. However, in many cases (far from the laser threshold), population densities are poorly affected by light emission and propagation, being fixed by external pumping. We also observe that Eq. (10) has a structure analogous to the corresponding equation describing emission from thermal sources [7, 8].

To assess the power and versability of the proposed scheme, we investigate the field-intensity distribution around a fluorescent low-symmetry nano-structured system. We consider first a pair of 3D emitting quavers with uniform composition (relative dielectric constant $\varepsilon = 8.9 + 0.5i$) and population densities. The size of the whole structure is 450×380 nm and its height is 30 nm. Fig. 1 (a) displays $\mathcal{I}(x, y, \bar{z}, \omega)$ in the proximity of the emitting

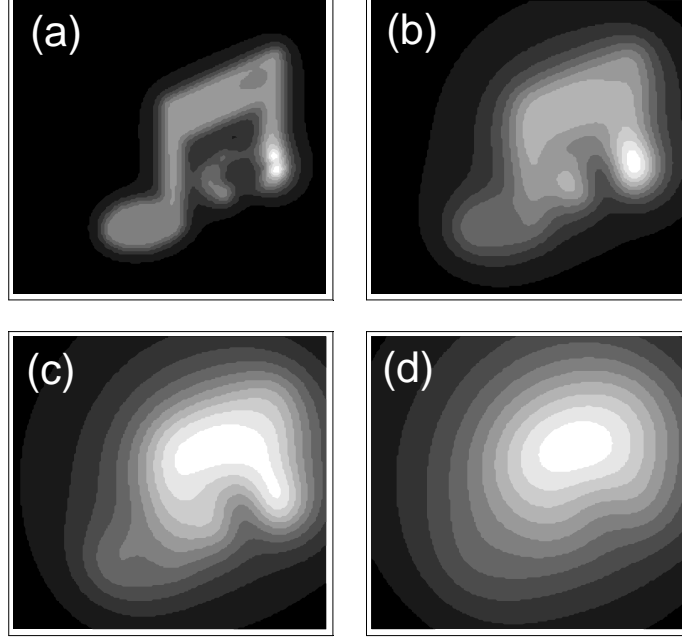


FIG. 3: The field intensity $\mathcal{I}(\mathbf{r}, \omega)$ (a) and partial intensities $\mathcal{I}_l(\mathbf{r}, \omega)$ for the structure with the metallic pad; (b) \mathcal{I}_x , (c) \mathcal{I}_y , (d) \mathcal{I}_z .

object in an observation plane located at $\bar{z} = 30$ nm. The Green tensor is computed by solving numerically a discretization of the Dyson equation [1]. Calculations have been made at $\lambda = 2\pi c/\omega = 600$ nm. The emission pattern reproduces almost perfectly the object shape (see also Fig. 2a where the structure is outlined). The light intensity is highest at the structure edges and nearby the smaller structures. Fig. 1b shows the effect of replacing the elliptic pad on the right of the structure with a silver pad. The emission pattern results to be significantly altered. In particular a strong enhancement of the field intensity nearby the edge of the silver pad is clearly observed while intensity is strongly depleted towards the pad center. This behaviour is typical of surface plasmons [9], in this case excited by the incoherent light originating from the nearby fluorescent structure.

The vector character of the emitted light is shown in Fig. 2. It displays the partial intensities $\mathcal{I}_l(\mathbf{r}, \omega)$ (i.e. the intensities that can be detected by a probe able to select light polarization) for the structure with the metallic pad. In spite of the isotropic character of the source currents, the three intensity distributions strongly differ one from each other. We observe that only \mathcal{I}_z reproduces quite well the object shape (except the metallic pad of course). Fig. 3 displays $\mathcal{I}(x, y, \bar{z}, \omega)$ for (a) $\bar{z} = 30$, (b) $\bar{z} = 60$, (c) $\bar{z} = 90$, and (d)

$\bar{z} = 150$ nm above the object. It shows how the relationship between near-field images and fluorescent objects is progressively lost at increasing observation distances.

We have proposed a general theoretical scheme for the investigation of light emitted from nano- and micrometric structures of arbitrary shape and composition. The presented numerical results provide useful guidelines for the interpretation of near-field photoluminescence spectroscopy/microscopy measurements. Moreover this theoretical and numerical scheme can be applied to the design of photonic systems with active elements.

We thank Omar Di Stefano for stimulating discussions.

-
- [1] O. J. F. Martin, C. Girard, and A. Dereux, Phys. Rev. Lett. **74**, 526 (1995).
 - [2] A. Madrazo and M. Nieto-Vesperinas, Appl. Phys. Lett. **70**, 31 (1997).
 - [3] S. Fan, I. Appelbaum, and J. D. Joannopoulos, Appl. Phys. Lett. **75**, 3461 (1999).
 - [4] J. D. Joannopoulos, R. D. Meade, and J. N. Winn, *Photonic Crystals*, (Princeton Univ. Press, 1995).
 - [5] S. Savasta, O. Di Stefano, and R. Girlanda, Phys. Rev. A **65**, 043801 (2002).
 - [6] C. H. Henry, and R. F. Kazarinov, Rev. Mod. Phys. **68**, 801 (1996).
 - [7] J. P. Mulet, K. Joulain, R. Carminati and J.-J. Greffet, Appl. Phys. Lett. , **82**, 1660 (1999).
 - [8] J.-J. Greffet, R. Carminati, K. Joulain, J. P. Mulet, S. P. Mainguy, and Y. Chen, Nature **416**, 6876 (2002).
 - [9] H. Raether, Surface Plasmons, (Springer Verlag Berlin 1988).

FIGURE CAPTIONS

Fig. 1

(a) Field-intensity distribution around a pair of nanoscopic emitting quavers with uniform composition and population densities; (b) as (a) but with the elliptic pad on the right of the structure replaced with a silver pad. The two calculations have been made at $\lambda = 600$ nm and on the observation plane located 30 nm above the structure.

Fig. 2

The field intensity $\mathcal{I}(\mathbf{r}, \omega)$ (a) and partial intensities $\mathcal{I}_l(\mathbf{r}, \omega)$ for the structure with the metallic pad; (b) \mathcal{I}_x , (c) \mathcal{I}_y , (d) \mathcal{I}_z .

Fig. 3

The field intensity \mathcal{I} calculated on observation planes at increasing distance from the structure; (a) $z = 30$ nm, (b) $z = 60$ nm, (c) $z = 90$ nm, (d) $z = 150$ nm.